

## Selectivity of the Polyspecific Cation Transporter rOCT1 Is Changed by Mutation of Aspartate 475 to Glutamate

VALENTIN GORBOULEV,<sup>1</sup> CHRISTOPHER VOLK,<sup>1</sup> PETRA ARNDT, AIDA AKHOUNDOVA, and HERMANN KOEPESELL

Anatomisches Institut, Bayerische Julius-Maximilians-Universität, Würzburg, Germany

Received May 24, 1999; accepted August 20, 1999

This paper is available online at <http://www.molpharm.org>

### ABSTRACT

After site-directed mutagenesis, the organic cation transporter rOCT1 was expressed in *Xenopus laevis* oocytes or human embryonic kidney cells and functionally characterized. rOCT1 belongs to a new family of polyspecific transporters that includes transporters for organic cations and anions and the Na<sup>+</sup>-carnitine cotransporter. When glutamate was substituted for Asp475 (middle of the proposed 11th transmembrane  $\alpha$ -helix), the  $V_{\max}$  values for choline, tetraethylammonium (TEA), *N*<sup>1</sup>-methylnicotinamide, and 1-methyl-4-phenylpyridinium were reduced by 89 to 98%. The apparent  $K_m$  values were also decreased (choline by 15-fold, TEA by 8-fold, *N*<sup>1</sup>-methylnicotinamide by 4-fold) or remained constant (1-methyl-4-phenylpyridinium). After the mutation, the membrane potential dependence of the  $K_m$  value for [<sup>3</sup>H]choline uptake was abolished.

The affinity of *n*-tetraalkyl ammonium compounds to inhibit TEA uptake was increased. This affinity and its increase by the D475E mutation were increased with the length of the *n*-alkyl chains. After expression in *X. laevis* oocytes, the IC<sub>50</sub> ratios of wild-type and D475E mutant were 1.7 (tetramethylammonium), 4.3 (TEA), 5.0 (tetrapropylammonium), 5.0 (tetrabutylammonium), and 65 (tetrapentylammonium). Cationic inhibitors with ring structures were differentially affected: the IC<sub>50</sub> value for TEA inhibition by cyanine 863 remained unchanged, whereas it was increased for quinine. The data suggest that rOCT1 contains a large cation-binding pocket with several interaction domains that may be responsible for high-affinity binding of structurally different cations and that Asp475 is located close to one of these interaction domains.

A variety of polyspecific transporters responsible for excretion and reabsorption of drugs have been identified in eukaryotic plasma membranes. In addition to the P-glycoproteins (multidrug resistant) and multidrug resistance proteins, which are primary active export pumps (Fykse and Fonnum, 1991; Leier et al., 1994; Müller and Jansen, 1997), three families of polyspecific import transporters have been identified: the proton-peptide symporters (Meredith and Boyd, 1995), a family containing different organic anion transporters and the prostaglandin transporter (Kanai et al., 1995; Saito et al., 1996; Müller and Jansen, 1997), and the OCT1 family, which contains polyspecific cation and anion transporters (Koepsell, 1998; Koepsell et al., 1999). In 1994, we cloned rOCT1 (Gründemann et al., 1994), a transporter expressed in the basolateral membrane of hepatocytes (Meyer-Wentrup et al., 1998) and renal proximal tubules (unpublished data), which is responsible for the first step in hepatic and renal cation excretion. This transporter mediates the electrogenic uptake of a variety of small organic cations,

including many cationic drugs, choline, and monoamine neurotransmitters, and operates independently of sodium ions and proton gradients (Busch et al., 1996a,b). rOCT1 may translocate small cations in both directions, whereas large organic cations, such as quinine and cyanine 863, are high-affinity transport inhibitors but are themselves not transported (Nagel et al., 1997). OCT2 and OCT3 transporters are highly homologous subtypes of rOCT1 that operate in a similar fashion (Koepsell et al., 1999); these transporters are also electrogenic transporters of small cations, including the monoamine neurotransmitters, but they exhibit differences in substrate specificity (Koepsell et al., 1999). Another subgroup of the OCT1 family are the transporters OCTN1 and OCTN2, which translocate cations and zwitterions (Tamai et al., 1997; Wu et al., 1998). OCTN2 mediates Na<sup>+</sup>-dependent, high-affinity uptake of carnitine (Tamai et al., 1998), and gene defects in this transporter result in a systemic carnitine deficiency in mice and humans (Nezu et al., 1999).

It is of high medical significance that the molecular mechanism by which polyspecific transporters translocate a variety of structurally different substrates without losing substrate selectivity is elucidated. The tertiary structure of polyspecific transporters is unlikely to be resolved in the near

This work was supported by Deutsche Forschungsgemeinschaft Grant SFB 174/A22.

<sup>1</sup> V.G. and C.V. contributed equally to the work.

**ABBREVIATIONS:** TM, transmembrane  $\alpha$ -helix; HEK, human embryonic kidney; TMA, tetramethylammonium; TEA, tetraethylammonium; TPA, tetrapropylammonium; TBA, tetrabutylammonium; TPpA, tetrapentylammonium; MPP, 1-methyl-4-phenylpyridinium; NMN, *N*<sup>1</sup>-methylnicotinamide.

future, so we attempted to mutate amino acid residues in rOCT1 that may be involved in cation transport. rOCT1 represents an ideal model because more than 20 members of the OCT1 family have been cloned, including subfamilies that transport zwitterionic or negatively charged substrates. This provides a good basis to select amino acid residues for site-directed mutagenesis. Previously cloned members of the OCT1 family share a common predicted topology of 12 transmembrane  $\alpha$ -helices (TM) and one large extracellular loop between TM1 and TM2 (Koepsell et al., 1999). We decided to start our mutagenesis program by mutating glutamate and aspartate residues because the involvement of acidic amino acids in the translocation of cationic substrates has been demonstrated for bacterial and mammalian transporters (Wilson and Wilson, 1992; Yamaguchi et al., 1992; Pourcher et al., 1993). The mammalian transporters include the vesicular monoamine transporters (Merickel et al., 1995; Steiner-Mordoch et al., 1996), the vesicular acetylcholine transporter (Song et al., 1997; Kim et al., 1999), and the dopamine transporter (Kitayama et al., 1992). An amino acid sequence comparison demonstrated that the electrogenic cation transporters (OCT1, OCT2, and OCT3) contain six acidic amino acids that are conserved in neither the OCTN-type transporters nor the anion transporters: two glutamate (Glu68, Glu69) and two aspartate (Asp95, Asp150) residues in the large extracellular loop, one aspartate (Asp379) in TM8, and another (Asp475) in TM11. We began with the mutation of Asp475, located in the middle of TM11. Replacement of Asp475 by arginine, asparagine, and glutamate resulted in a significant reduction in the transport rate. Interestingly, after the mutation of Asp475 to glutamate, the affinity for specific cations was dramatically increased.

## Experimental Procedures

**Site-Directed Mutagenesis.** Mutants of rOCT 1 were constructed using the polymerase chain reaction approach either according to Chen and Przybyla (1994) or by use of the overlap extension method (Ho et al., 1989). The mutagenic primers were 5'-T GCC CTG TGT CGA CTG GGT GGG AT-3' (forward) for D475R, 5'-T GCC CTG TGT AAC CTG GTG GG-3' (forward) and 5'-C ACC CAG GTT ACA CAG GGC AG-3' (reverse) for D475N, and 5'-CC CTG TGT GAG CTC GGT GGG ATC TT-3' (forward) and 5'-A GAT CCC ACC GAG CTC ACA CAG GGC-3' (reverse) for D475E. Nucleotides corresponding to the mutated amino acid are underlined. The flanking primers were 5'-AGA CTG GCG CTG GCT CCA-3' (forward, position 817–834 of rOCT1) and 5'-GGT ACT TGA GGA CTT GCC-3' (reverse, position 1688–1705 of rOCT1). The polymerase chain reaction products were digested with *Sau*I and *Sty*I, and a 520-bp fragment was cloned into plasmid rOCT1/pRSSP (Busch et al., 1996b) cut with the same enzymes. The sequences of the cloned fragments were verified by DNA sequencing.

**Expression of rOCT1 in Oocytes of *Xenopus laevis* and Transport Measurements.** The experiments with *X. laevis* oocytes were performed as described previously (Gründemann et al., 1994; Busch et al., 1996b). Briefly, the oocytes were stored in 5 mM 3-(*N*-morpholino)propanesulfonic acid-NaOH, pH 7.4, 100 mM NaCl, 1 mM MgCl<sub>2</sub>, 3 mM KCl, and 2 mM CaCl<sub>2</sub> (Ori buffer) containing 50 mg/liter gentamicin. Oocytes were injected with 10 ng of cRNA and incubated for 2 or 3 days at 19°C in Ori buffer. For tracer uptake measurements, oocytes were incubated for 60 min at 19°C in Ori buffer containing radioactively labeled cations. The incubation was performed in the absence and presence of 50  $\mu$ M cyanine 863, and the cyanine-inhibited uptake was calculated. The uptake of the analyzed cations into the oocytes was linear during this time period. In

some measurements, sodium in the Ori buffer was replaced by potassium or different concentrations of nonradioactive substrates or inhibitors were added. The transport was stopped with ice-cold Ori buffer, and the oocytes were washed four times with ice-cold Ori buffer, solubilized with 100  $\mu$ l of 5% (w/v) SDS, and analyzed for radioactivity. Membrane potential measurements or two-electrode voltage-clamp recordings in *X. laevis* oocytes were performed as described previously (Nagel et al., 1997). The oocytes were permanently superfused with fresh Ori buffer at room temperature (3 ml/min). In some experiments, NaCl was replaced by KCl to change the membrane potential.

**Preparation of Plasma Membranes from *X. laevis* Oocytes and Western Blot Analysis.** *X. laevis* oocytes were injected with water (controls) or with 10 ng of cRNA of rOCT1, D475R, D475N, or D475E and incubated for 3 days at 19°C. Half of the oocytes were used for uptake measurements. The plasma membranes of the other half of the oocytes (~60) were isolated through differential centrifugations at 1,000g and 10,000g according to Geering et al. (1989). For Western blot analysis, 3 to 6  $\mu$ g of isolated plasma membranes were incubated for 30 min at 37°C in 60 mM Tris · HCl, pH 6.8, 100 mM dithiothreitol, 2% (w/v) SDS, and 7% (v/v) glycerol; resolved by SDS-polyacrylamide gel electrophoresis; transferred to nitrocellulose; and incubated with antibody raised against the large extracellular loop of rOCT1 as described previously (Meyer-Wentrup et al., 1998). Reaction with the peroxidase-conjugated secondary antibody (goat anti-rabbit IgG) was visualized by enhanced chemiluminescence (ECL system; Amersham Buchler; Braunschweig, Germany). Prestained molecular weight marker BenchMark (Life Technologies, Karlsruhe, Germany) was used to determine apparent molecular masses.

**Transient Expression in Human Embryonic Kidney (HEK) 293 Cells.** HEK 293 cells were grown in Dulbecco's modified Eagle's medium with 10% FCS, and the cells were transfected with the empty vector pRcCMV (InVitrogen, Groningen, the Netherlands) or with pRcCMV containing rOCT1, D475R, D475N, or D475E using the FuGENE 6 reagent from Boehringer-Mannheim Biochemica (Mannheim, Germany). When the cells became confluent 2 days after transfection, they were washed with PBS, suspended by shaking, collected by 10-min centrifugation at 1000g, and suspended at 37°C in PBS. For uptake measurements, the cells were suspended for 1 to 20 s with PBS (37°C) that contained either different concentrations of 1-[<sup>3</sup>H]methyl-4-phenylpyridinium ([<sup>3</sup>H]MPP) without and with 50  $\mu$ M cyanine 863 or 0.1  $\mu$ M [<sup>3</sup>H]MPP without and with different concentrations of tetrapentylammonium (TPeA). The uptake reactions were stopped with ice-cold PBS containing 100  $\mu$ M quinine (stop solution), and the cells were washed three times by 5-min centrifugation with the ice-cold stop solution. In the stop solution, no significant cation efflux from the cells could be observed.

**Calculations and Statistics.** Indicated uptake rates from *X. laevis* oocytes represent medians from pairs of 8 to 10 oocytes  $\pm$ S.E. values. The uptake rates determined in HEK 293 cells represent mean values from pairs of three or four determinations  $\pm$ S.D. Apparent  $K_m$  values were calculated by fitting the Michaelis-Menten equation to uptake measurements at different substrate concentrations. For calculation of IC<sub>50</sub> values, the Hill equation for multisite inhibition was fitted to the data.

**Materials.** [<sup>3</sup>H]MPP (2.2 TBq/mmol) was provided by Biotrend (Köln, Germany). The other materials were obtained as described previously (Busch et al., 1996b).

## Results

To elucidate the role of Asp475 in rOCT1 for the transport of organic cations, we changed this residue to arginine (D475R), asparagine (D475N), or glutamate (D475E) and expressed the mutants in *X. laevis* oocytes and HEK 293 cells. Oocytes were injected with 10 ng of cRNA, and the uptake rates of 10  $\mu$ M [<sup>14</sup>C]TEA and 0.1  $\mu$ M [<sup>3</sup>H]MPP were

determined in the absence and presence of 50  $\mu\text{M}$  cyanine 863. In one batch of oocytes, the cyanine-inhibited uptake rates of TEA were  $30.1 \pm 3.8$  (wild type),  $0.06 \pm 0.08$  (D475R),  $0.32 \pm 0.14$  (D475N),  $7.1 \pm 2.8$  (D475E), and  $0.31 \pm 0.05$  ( $\text{H}_2\text{O}$ )  $\text{pmol} \cdot \text{oocyte}^{-1} \cdot \text{h}^{-1}$ . The uptake rates in the presence of 50  $\mu\text{M}$  cyanine were  $0.03 \pm 0.01$  (wild type),  $0.09 \pm 0.03$  (D475R),  $0.09 \pm 0.06$  (D475N),  $0.06 \pm 0.03$  (D475E), and  $0.01 \pm 0.01$  ( $\text{H}_2\text{O}$ )  $\text{pmol} \cdot \text{oocyte}^{-1} \cdot \text{h}^{-1}$ . After transfection in HEK 293 cells, cyanine-inhibitable [ $^3\text{H}$ ]MPP uptake could be expressed with all three D475 mutants (Fig. 1). At variance with wild-type rOCT1, cyanine-inhibited [ $^3\text{H}$ ]MPP uptake in the mutants was linear for about 10 s. For 0.1  $\mu\text{M}$  [ $^3\text{H}$ ]MPP, cyanine-inhibited initial uptake rates of  $280 \pm 10$  (wild type),  $15 \pm 2$  (D475R),  $20 \pm 1$  (D475N),  $22 \pm 1$  (D475E), and  $4 \pm 1$  (empty pRCMV plasmid)  $\text{fmol} \cdot \text{mg}^{-1} \cdot \text{s}^{-1}$  were determined. In the presence of 50  $\mu\text{M}$  cyanine 863, the uptake rates were  $25 \pm 11$  (wild type),  $2.9 \pm 0.9$  (D475R),  $8.8 \pm 1.0$  (D475N), and  $3.0 \pm 0.4$  (D475E)  $\text{fmol} \cdot \text{mg}^{-1} \cdot \text{s}^{-1}$ . To investigate whether the mutations disturb the insertion of rOCT1 into the plasma membrane, we probed Western blots with plasma membranes isolated from *X. laevis* oocytes and reacted nonpermeabilized HEK 293 cells with an affinity-purified antibody against the large extracellular loop of rOCT1 (Meyer-Wentrup et al., 1998). Different results were obtained with the two expression systems. Figure 2 shows Western blots of plasma membrane fractions from oocytes that were developed with a specific antibody against rOCT1. With wild-type rOCT1 and the D475R mutant, two immunoreactive polypeptide bands with apparent molecular masses of 52 and 60 to 70 kDa were observed, which represent differentially glycosylated transporter proteins (unpublished data). After expression of the D475R and D475E mutants, greater protein amounts were observed in the plasma membrane fraction than in the wild type, and the 60- to 70-kDa polypeptide was not detected in the D475E mutant (Fig. 2). In three independent experiments with different mRNA preparations and oocyte batches, the D475N mutant could not be detected in the plasma membrane fraction, although the cRNA of the D475N mutant was

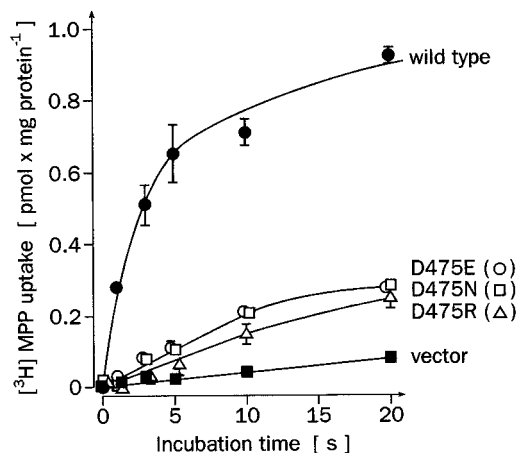


**Fig. 1.** Expression of MPP uptake in HEK 293 cells by wild-type rOCT1 and mutants of Asp475. HEK 293 cells were transiently transfected with the pRCMV vector containing wild-type rOCT1 or the mutant D475E, D475N, or D475R. As control, the cells were transfected with the empty vector. At 2 days after the transfection, the uptake of 0.1  $\mu\text{M}$  [ $^3\text{H}$ ] MPP was measured in the absence and presence of 50  $\mu\text{M}$  cyanine 863. The cyanine-inhibited uptake is presented. Mean  $\pm$  S.D. values from three parallel measurements are shown.

shown to display a similar stability in the oocytes as wild-type cRNA. In contrast to the oocyte experiments, immunohistochemistry with HEK 293 cells indicated that all three mutants were inserted into the plasma membrane because the antibody against the large extracellular loop of rOCT1 showed a significant reaction with nonpermeabilized cells expressing the D475R, D475E, and D475N mutants (Fig. 3). No immunoreaction was observed with vector-transfected control cells. On visual inspection of three experiments, we did not distinguish differences in the immunoreaction of transfected wild-type rOCT1 and the mutants.

To elucidate the functional role of Asp475, we compared functional properties and substrate specificity of the D475E mutant with those of the wild-type rOCT1. Because the  $K_m$  values are potential dependent (Busch et al., 1996b) and the membrane potential varies with different batches of *X. laevis* oocytes, the functional characteristics of the D475E mutant and wild type were compared within the same batches of oocytes. Figure 4 shows the substrate dependence of the cyanine 863-inhibited uptake of TEA,  $N^1$ -methylnicotinamide (NMN), choline, and MPP. Fitting the Michaelis-Menten equation to the data, the following  $K_m$  values were obtained for the wild type and mutant, respectively: TEA,  $129 \pm 17$  versus  $16 \pm 4$   $\mu\text{M}$ ; NMN,  $126 \pm 20$  versus  $35 \pm 5$   $\mu\text{M}$ ; choline,  $370 \pm 120$  versus  $25 \pm 7$   $\mu\text{M}$ ; and MPP,  $2.7 \pm 1.1$   $\mu\text{M}$  versus  $2.2 \pm 0.9$   $\mu\text{M}$ . The data indicate that the mutation of Asp475 to glutamate leads to a significant decrease in  $K_m$  values of several small organic cations. However, the  $K_m$  value of the more bulky cation MPP was not changed. In the D475E mutant, the  $V_{\text{max}}$  values for transport were drastically reduced compared with that of the wild type: to 2.3% for TEA, 3.2% for NMN, 3.5% for choline, and 11.4% for MPP. The data show that the D475E mutation alters the affinity for some of the transported cations.

Most bulky cations, such as quinine, *d*-tubocurarine, and cyanine 863, are high-affinity inhibitors of rOCT1-mediated cation uptake but are not transported (Nagel et al., 1997). Recently, we found that TPcA belongs to this group of non-transported inhibitors and that quinine, cyanine 863, and TPcA inhibited the uptake of [ $^{14}\text{C}$ ]TEA in a noncompetitive manner (unpublished data). Because the D475E mutation apparently altered the structure of the substrate binding

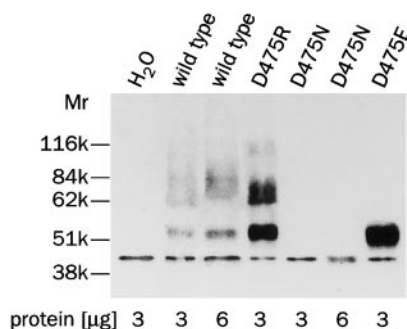


**Fig. 2.** Targeting of rOCT1 mutants to plasma membrane in *X. laevis* oocytes. *X. laevis* oocytes were injected with water, cRNA of wild-type rOCT1, or cRNAs of the indicated mutants. After a 3-day incubation, plasma membranes were isolated, and the indicated amounts of membrane protein were separated by SDS-polyacrylamide gel electrophoresis. Western blots are shown that were developed with a polyclonal antibody raised against the large extracellular loop of rOCT1. Antibody reaction with rOCT1 was mainly observed at about 52 kDa and between 60 and 70 kDa.



site, we performed inhibition experiments with transported cations and noncompetitive cationic inhibitors to determine whether the D475E mutation has an effect on both types of cationic interactions. To systematically investigate the cation interaction, we measured the transport inhibition by *n*-tetraalkyl ammonium compounds with increasing chain length (Wright et al., 1995). In Fig. 5, we sought to determine the quaternary ammonium compounds that were transported. When *X. laevis* oocytes expressing wild-type rOCT1 clamped at  $-50$  mV were superfused with saturating concentrations (Fig. 6) of tetramethylammonium (TMA), TEA, tetrapro-

pylammonium (TPA), tetrabutylammonium (TBA), or TPeA, significant rOCT1-mediated inward currents were detected only with TMA and TEA. Because the TMA-induced current by rOCT1 increased with increasing membrane potential (data not shown), we conclude that TMA is also transported by rOCT1. The small inward currents observed with TPA, TBA, and TPeA were similar to those observed with noninjected control oocytes (Fig. 5). Thus, TPA, TBA, and TPeA do not mediate a significant charge transport. These cations may be transported very slowly, without netto translocation of electric charge, or they may be nontransported inhibitors. Dose-response curves for inhibition of TEA transport expressed by wild-type rOCT1 and the D475E mutant are shown in Fig. 6. The affinity of the *n*-tetraalkyl ammonium compounds increased with increasing alkyl chain length. In the wild type, the  $IC_{50}$  values for inhibition decreased from  $1.3 \pm 0.4$  mM (TMA),  $81 \pm 9$   $\mu$ M (TEA),  $12 \pm 5$   $\mu$ M (TPA),

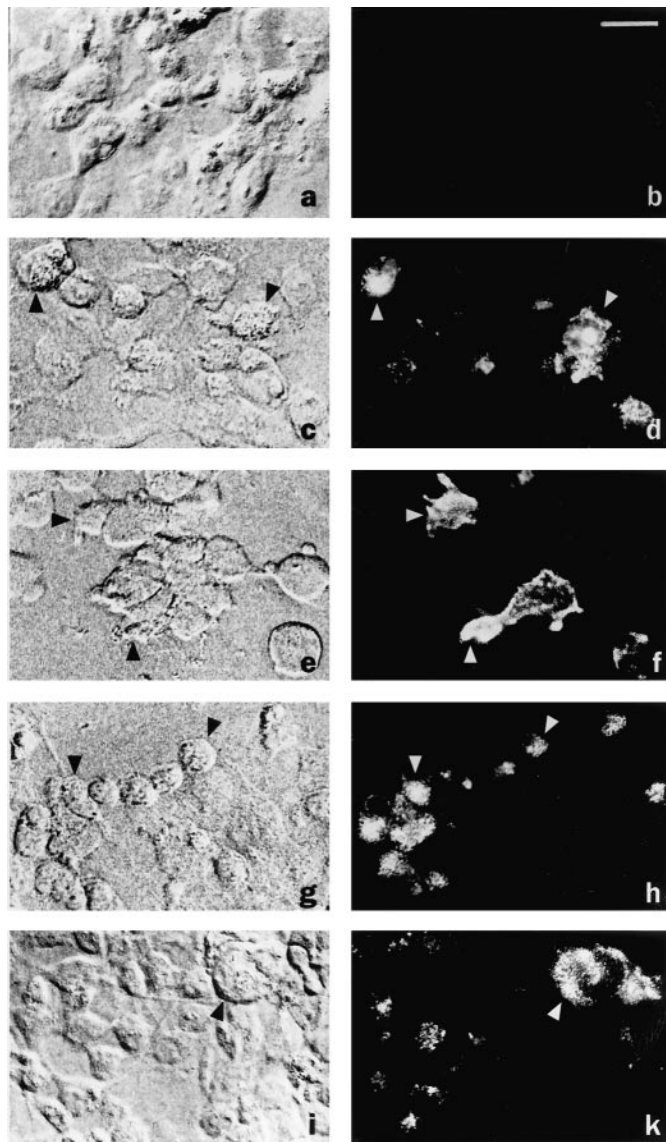


**Fig. 3.** Targeting of rOCT1 mutants to plasma membrane in HEK 293 cells, which were transiently transfected with the empty pRcCMV vector (a and b) or with the pRcCMV vector containing rOCT1 (c and d), D475R (e and f), D475N (g and h), or D475E (i and k), seeded onto glass slides and grown for 2 days. The cells were fixed with 4% (v/v) paraformaldehyde and washed with PBS. The immunoreaction was performed with the affinity-purified antibody against the large extracellular loop of rOCT1. Under these conditions, the cells were nonpermeabilized, and no antibody reaction could be observed with an antibody against the intracellular carboxyl terminus (data not shown). Identical areas are presented that were visualized by phase contrast microscopy (left) and immunofluorescence (right). Some immunoreactive cells are indicated by arrowheads. Bar, 25  $\mu$ M.

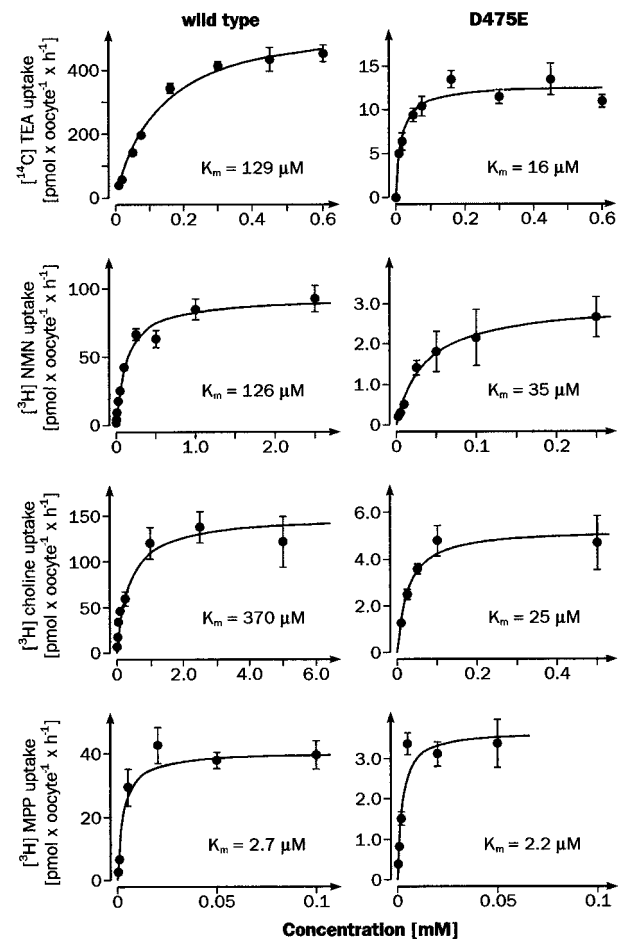


**Fig. 4.** The substrate dependence for some cations after expression of rOCT1 and the D475E mutant in *X. laevis* oocytes. rOCT1 cRNA or cRNA from D475E mutant was injected into identical batches of *X. laevis* oocytes, and parallel transport measurements for each of the indicated substrates were performed with the wild type and mutant. Uptake of different concentrations of [ $^{14}$ C]TEA, [ $^3$ H]NMN, [ $^3$ H]choline, and [ $^3$ H]MPP was measured in the absence and presence of 50  $\mu$ M cyanine 863, and the cyanine-inhibitable uptake rates were calculated. Median  $\pm$  S.E. values from pairs of 8 to 10 individual oocytes are presented, and the Michaelis-Menten equation was fitted to the data. The  $K_m$  values are indicated. For the wild type and mutant, the following  $V_{max}$  values were obtained (in pmol  $\cdot$  oocyte $^{-1} \cdot$  h $^{-1}$ ): TEA,  $569 \pm 27$  and  $13 \pm 0.7$ ; NMN,  $94 \pm 4$  and  $3.0 \pm 0.2$ ; choline,  $150 \pm 12$  and  $5.3 \pm 0.4$ ; and MPP,  $41 \pm 3$  and  $4.6 \pm 0.5$ .

and  $3.0 \pm 2.0 \mu\text{M}$  (TBA) to  $0.53 \pm 0.04 \mu\text{M}$  (TPeA), and in the D475E mutant, the  $\text{IC}_{50}$  values decreased from  $0.78 \pm 0.12 \text{ mM}$  (TMA),  $19 \pm 5 \mu\text{M}$  (TEA),  $2.4 \pm 0.3 \mu\text{M}$  (TPA), and  $0.6 \pm 0.2 \mu\text{M}$  (TBA) to  $0.008 \pm 0.002 \mu\text{M}$  (TPeA). The *n*-tetraalkyl ammonium compounds had a higher affinity for the D475E mutant than for the wild type, and the effect of the mutation increased with increasing alkyl chain length: the ratios between the  $\text{IC}_{50}$  values of the wild type and D475E mutant were 1.7 (TMA), 4.3 (TEA), 5.0 (TPA), 5.0 (TBA), and 65 (TPeA). Next, we compared the rOCT1 wild type and D475E mutant for inhibition of TEA uptake by the noncompetitive inhibitors cyanine 863, quinine, and quinidine, which contain bulky ring structures. Although the affinity of cyanine 863 was not changed by the D475E mutation (Fig. 6;  $\text{IC}_{50} = 1.8 \pm 0.6 \mu\text{M}$  for wild type and  $2.0 \pm 0.4 \mu\text{M}$  for D475E mutant), the affinity of quinidine may be increased slightly ( $\text{IC}_{50} = 4.2 \pm 0.7 \mu\text{M}$  for wild type and  $2.8 \pm 0.5 \mu\text{M}$  for D475E mutant, difference not significant), and the affinity of quinine was decreased ( $\text{IC}_{50} = 0.57 \pm 0.04 \mu\text{M}$  for wild type and  $1.3 \pm 0.3 \mu\text{M}$  for D475E mutant,  $P < .05$ ). Thus, the D475E mutation impairs the stereoselective interaction of quinine and quinidine with rOCT1 (Busch et al., 1996b).

Through measurement of choline-induced currents in rOCT1 expressing voltage-clamped *X. laevis* oocytes, we previously observed that the choline concentrations required to induce half-maximal currents decreased at higher membrane potentials (Busch et al., 1996b). Because the low transport activity of the D475E mutant did not allow an electrical analysis, we measured the substrate dependence of [ $^3\text{H}$ ]choline uptake with  $100 \text{ mM Na}^+$  in the bath and after replacement of  $\text{Na}^+$  with  $\text{K}^+$ ; the membrane potential decreased from  $-34 \pm 3.9 \text{ mV}$  ( $n = 5$ ) to  $-13.6 \pm 1.0 \text{ mV}$  ( $n = 5$ ). The apparent  $K_m$  value for cyanine-inhibitable choline transport by rOCT1 increased from  $0.23 \pm 0.04 \text{ mM}$  with sodium to  $1.14 \pm 0.23 \text{ mM}$  after the replacement of sodium with potas-

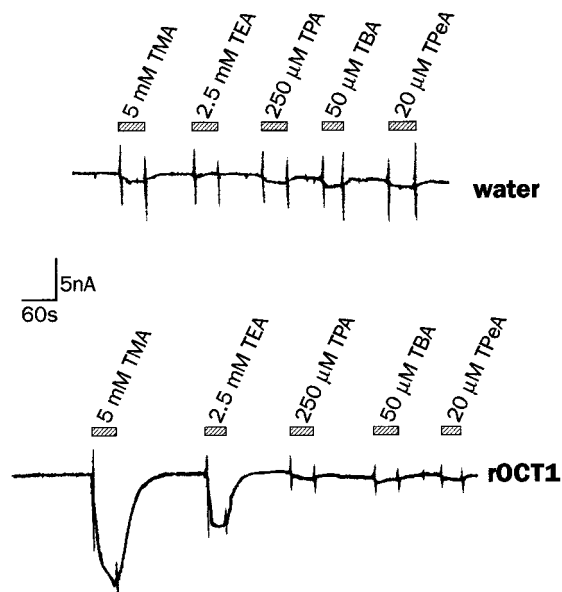


**Fig. 5.** Induction of current changes by transported quaternary *n*-alkyl ammonium salts in *X. laevis* oocytes expressing wild-type rOCT1. After injection of water or wild-type rOCT1 cRNA, *X. laevis* oocytes were voltage-clamped to  $-50 \text{ mV}$  and superfused with Ori buffer containing the indicated concentrations of *n*-tetraalkyl ammonium compounds. The induced currents are shown.

sium, whereas the  $V_{\text{max}}$  value was not changed (Fig. 7a). In the D475E mutant, the effect of the membrane potential on the  $K_m$  value was abolished: the apparent  $K_m$  values with sodium and potassium in the bath were  $15 \pm 3$  and  $17 \pm 6 \mu\text{M}$ , respectively (Fig. 7b). At variance to wild-type rOCT1, the  $V_{\text{max}}$  value of choline transport expressed by the D475E mutant was reduced in the presence of  $\text{K}^+$ . The data show that the potential dependence of choline binding to rOCT1 is changed by the D475E mutation.

Next, we investigated whether specific effects of the D475E mutation on cation affinity observed in the oocyte expression system could be also detected when the transporter was expressed in mammalian epithelial cells. In Fig. 8, we compared the substrate dependence of [ $^3\text{H}$ ]MPP uptake into HEK 293 cells that were either transfected with wild-type rOCT1 or with the D475E mutant. For cyanine-inhibited MPP uptake by wild-type rOCT1 and by the D475E mutant, nearly identical  $K_m$  values of  $9.4 \pm 0.1$  (wild type) and  $9.3 \pm 1.1 \mu\text{M}$  (D475E) were obtained as has been observed in *X. laevis* oocytes. The  $K_m$  value for cyanine-inhibited MPP uptake also was not changed significantly when Asp475 was replaced by arginine or asparagine. For these mutants,  $K_m$

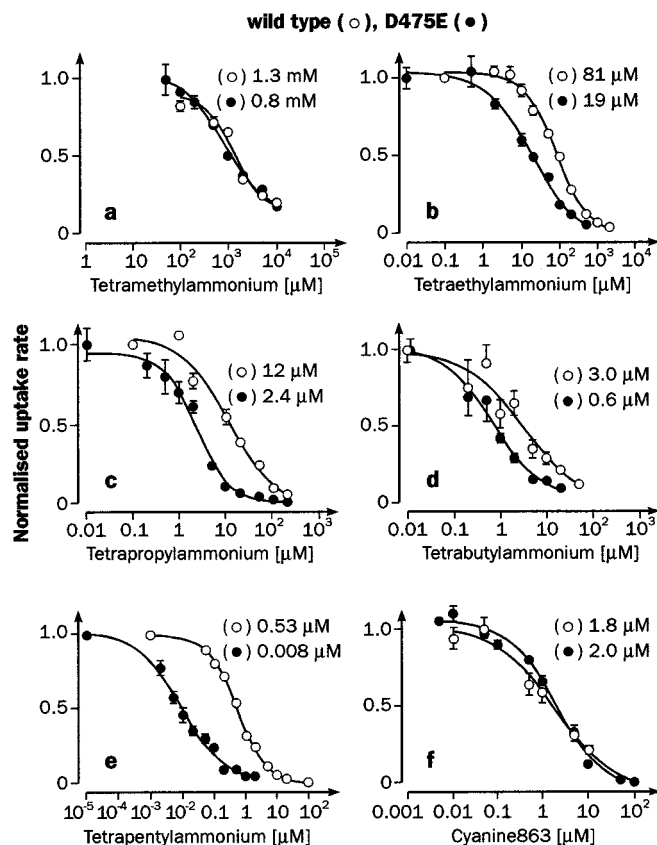


**Fig. 6.** Inhibition of TEA uptake expressed in *X. laevis* oocytes by transported and nontransported inhibitory cations. Different batches of *X. laevis* oocytes (a–f) were injected with cRNA of rOCT1 or the D475E mutant. After a 3-day incubation, the uptake of  $10 \mu\text{M}$  [ $^3\text{H}$ ]TEA was measured in the presence of the different concentrations of TMA, TEA, TPA, TBA, TPeA, or cyanine 863. ○, uptake measurements with wild-type rOCT1. ●, parallel measurements with the D475E mutant. The median and S.E. values of 8 to 10 oocytes are shown. The indicated  $\text{IC}_{50}$  values were obtained by fitting the Hill equation to the data. The differences between the  $\text{IC}_{50}$  values obtained for the inhibition of wild type and mutant were significantly different, with the exception of TMA and cyanine 863.

values of  $5.8 \pm 2.4 \mu\text{M}$  (D475R) and  $10.6 \pm 3.2 \mu\text{M}$  (D475N) were determined. The differences between the  $K_m$  values after the expression of rOCT1 in *X. laevis* oocytes or HEK 293 cells may be due to differences in intracellular concentrations of endogenous cations or to different degrees of post-translational modifications. The  $V_{\max}$  values of cyanine-inhibited MPP uptake expressed by rOCT1 wild type and D475E mutant were  $12.1 \pm 0.5$  and  $0.075 \pm 0.003 \text{ pmol} \cdot \text{mg protein}^{-1} \cdot \text{s}^{-1}$ , respectively. This suggests that the turnover number for MPP transport by rOCT1 is reduced by the D475E mutation.

We determined whether the affinity change for *n*-alkyl ammonium compounds by the D475E mutation that was observed after expression of the transporter in *X. laevis* oocytes could be also detected in HEK 293 cells. Figure 9 shows rOCT1-mediated dose-response curves for the inhibition of [ $^3\text{H}$ ]MPP transport by TPcA in these cells. For the initial cyanine-inhibited uptake rates of [ $^3\text{H}$ ]MPP expressed by wild-type rOCT1 or by the D475E mutant,  $\text{IC}_{50}$  values of  $0.18 \pm 0.04$  and  $0.018 \pm 0.001 \mu\text{M}$  were determined, respectively. The data show that the affinity increase by the D475E mutation can be observed in different expression systems.

## Discussion

The data indicate that Asp475 in the presumed 11th membrane spanning  $\alpha$ -helix of rOCT1 is important for cation selectivity. After the expression of rOCT1 in HEK 293 cells, cation transport was largely reduced when Asp475 was re-

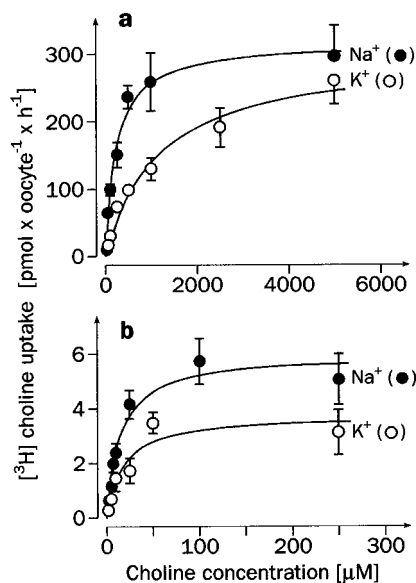


**Fig. 7.** Test of choline uptake by rOCT1 or by the D475E mutant for potential dependence. *X. laevis* oocytes were injected with cRNA of rOCT1 (a) with cRNA of the D475E mutant (b) or with water, and uptake of different [ $^3\text{H}$ ]choline concentrations in the absence and presence of  $50 \mu\text{M}$  cyanine 863 was measured in Ori buffer containing  $100 \text{ mM Na}^+$  (●) or in Ori buffer where  $\text{Na}^+$  was replaced by  $\text{K}^+$  (○). The cyanine-inhibitable uptake rates were calculated from pairs of 8 to 10 oocytes, and median and S.E. values are presented. In the water-injected control oocytes, the cyanine-inhibitable choline uptake measured at choline concentrations of 1 and 5 mM was less than  $0.9 \text{ pmol} \cdot \text{oocyte}^{-1} \cdot \text{h}^{-1}$ . The presented curves were obtained by fitting the Michaelis-Menten equation to the data. The following  $K_m$  values (in mM) and  $V_{\max}$  values (in  $\text{pmol} \cdot \text{oocyte}^{-1} \cdot \text{h}^{-1}$ ) were calculated: wild-type  $K_m(\text{Na})$ ,  $0.23 \pm 0.04$ ; wild-type  $K_m(\text{K})$ ,  $1.14 \pm 0.23$ ; wild-type  $V_{\max}(\text{Na})$ ,  $318 \pm 23$ ; wild-type  $V_{\max}(\text{K})$ ,  $303 \pm 23$ ; D475E  $K_m(\text{Na})$ ,  $0.015 \pm 0.003$ ; D475E  $K_m(\text{K})$ ,  $0.017 \pm 0.006$ ; D475E  $V_{\max}(\text{Na})$ ,  $6.0 \pm 0.4$ ; and D475E  $V_{\max}(\text{K})$ ,  $3.7 \pm 0.5$ .

placed by arginine, asparagine, or glutamate, although similar amounts of transporter proteins were targeted to the plasma membrane and a proper membrane insertion can be assumed because the extracellular localization of the large loop between the first and second presumed transmembranes was verified (Fig. 3). After expression of the mutants in *X. laevis* oocytes, transport activity was detected only with the D475E mutant. In the oocytes, the D475N mutant was not targeted to the oocyte plasma membrane, whereas the D475R

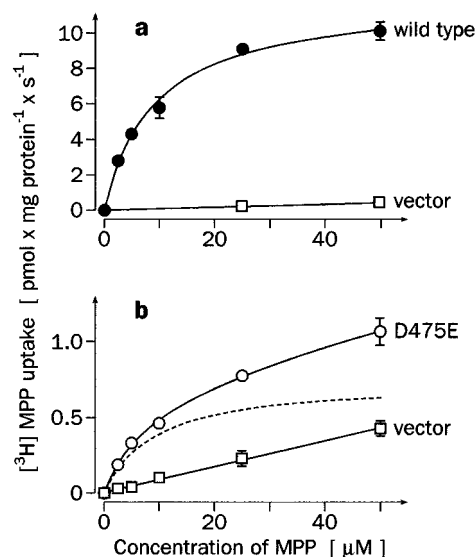


**Fig. 8.** Concentration dependence of MPP uptake after expression of rOCT1 and the D475E mutant in HEK 293 cells, which were transfected with the empty pRcCMV vector (□), with pRcCMV containing rOCT1 (●), or with pRcCMV containing the D475E mutant (○). After a 2-day incubation, initial uptake rates of [ $^3\text{H}$ ]MPP were measured by incubating the cells for 1 s (●) or 10 s (□, ○) with the indicated concentrations of MPP. The incubation was performed in the absence and presence of  $50 \mu\text{M}$  cyanine 863, and the cyanine-inhibited uptake rates were calculated. Mean  $\pm$  S.D. values from pairs of three parallel measurements are presented. The Michaelis-Menten equation plus a linear uptake component was fitted to the uptake rates obtained after expression of wild-type rOCT1 (●) or of the D475E mutant (○). The straight line for the uptake after transfection with the empty vector (□) was calculated by linear regression ( $r^2 > 0.99$ ). The dotted line was obtained when the Michaelis-Menten equation (without linear uptake component) was fitted to uptake rates that were measured after expression of the D475E mutant and corrected for uptake in vector-transfected control cells.

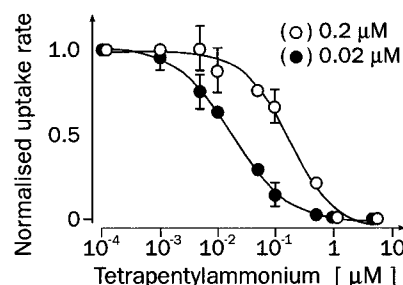


**Fig. 9.** Inhibition of MPP uptake by TPcA after expression of rOCT1 (○) and the D475E mutant (●) in HEK 293 cells. Two days after transfection of HEK 293 cells with the empty pRcCMV vector, wild-type rOCT1, or the D475E mutant, initial cyanine-inhibited uptake rates of  $0.1 \mu\text{M}$  [ $^3\text{H}$ ]MPP were measured in the presence of the indicated concentrations of TPcA. Mean  $\pm$  S.D. values of cyanine-inhibited uptake rates are shown. The values were calculated from pairs of three determinations and corrected for the cyanine-inhibited uptake rates in cells that had been transfected with the empty vector. The calculated  $\text{IC}_{50}$  values are indicated on the graph.



mutation may not be folded properly. The differences observed with the two expression systems are supposed to depend on differential post-translational modifications or on different regulatory states of the transporter. For example, the degree of glycosylation in the Golgi complex may be influenced by the conformation of the transporter, which may be stabilized by the binding of endogenous cations. Mutations in the substrate binding site may abolish this effect and may be one reason for changes in glycosylation. Recently, it was demonstrated that the glycosylation of the human multidrug resistance P-glycoprotein is highly dependent on the presence of intracellular substrates (Loo and Clarke, 1999).

Independent from the expression system, we observed that the functional properties of rOCT1 were significantly changed when Asp475 was replaced by glutamate, leading to an approximately 3 Å displacement of the negatively charged carboxyl group from the  $\alpha$ -helical backbone. This mutation resulted in a significant affinity increase for some transported cations (shown for TEA, NMN, and choline in oocytes), whereas the affinity of other transported cations (shown for MPP in oocytes and HEK 293 cells) remained unchanged. For wild-type rOCT1, the rank order of apparent  $K_m$  values was  $MPP \ll NMN = TEA < choline < TMA$ , whereas it was  $MPP < TEA < choline < NMN < TMA$  for the D475E mutant. Thus, the selectivity of transported cations was changed. By the D475E mutation, the  $V_{max}$  value of MPP uptake expressed in HEK 293 cells was reduced by 94%. Because our immunohistochemical data revealed similar amounts of wild-type rOCT1 and D475E mutant in the plasma membrane and the  $K_m$  value for MPP was not changed, the turnover for MPP is probably reduced in this mutant. By the D475E mutation, a similar reduction of the  $V_{max}$  for MPP uptake was observed in oocytes (by 89%) as in HEK 293 cells (by 94%). This suggests that the D475E mutant is properly targeted and folded in the oocytes. Interestingly, in the oocytes, the  $V_{max}$  values for uptake of TEA, NMN, and choline by the D475E mutant were reduced by 97 to 98%, which is significantly more than the  $V_{max}$  of MPP uptake. This suggests that the increased affinity of these cations leads to an impaired intracellular cation release that slows down the transport rate.

The organic cation transporter is a facilitated diffusion system for cations that may operate in both directions and can be driven by chemical cation gradient and/or the membrane potential (Busch et al., 1996b, 1998). According to current transporter models, substrate binding to an outwardly directed site may induce a conformational change in the transporter that makes the cation binding site accessible to the cytosol. Our data show that the mutation of Asp475 to glutamate alters the structure of the cation binding site and impairs the translocation step. This can be concluded from the observation that the  $V_{max}$  value for MPP transport was reduced, although the  $K_m$  value was not changed. We cannot distinguish whether Asp475 is localized within the cation binding site and transport pathway or whether Asp475 helps to shape these functional important transporter regions by stabilizing their tertiary structures. The observations that the affinity of rOCT1 for a variety of cations is increased by the D475E mutation and that the affinity increases with the alkyl chain length strongly suggest that Asp475 is localized close to the cation binding site because it is very unlikely that such distinct effects result from a long-range conformational

effect induced by a conservative point mutation. Thus, our data suggest either that Asp475 is located within the transport pathway at the cation binding site or that Asp475 is located at a nearby protein domain and stabilizes the conformation of the cation binding site through an ionic interaction with another intramembraneous protein domain. The finding that the mutation of Asp475 to glutamate impairs the potential dependence of the  $K_m$  value for choline transport further strengthens the functional importance of this amino acid residue. Further investigations are required to elucidate whether cation binding or cation release is potential dependent and which step during cation translocation is influenced by the membrane potential.

The organic cation transporters rOCT1, rOCT2, and rOCT3 translocate a variety of small cations and are inhibited by larger, more hydrophobic cations, such as quinine, cyanine 863, decynium, and TPeA (Nagel et al., 1997; Koepsell et al., 1999; present article). Recently, we showed that quinine, cyanine 863, decynium 22, and TPeA inhibit [ $^{14}C$ ]TEA uptake expressed by rOCT1 or rOCT2 in a noncompetitive manner (unpublished data). The observation that the D475E mutation in rOCT1 not only increases the affinity of transported cations but also increases the affinity of the noncompetitive inhibitor TPeA strongly suggests that transported and inhibitory cations interact at the same binding site because a point mutation should not alter the cation affinity of two different binding sites in the same way. The noncompetitive type of inhibition observed with the high-affinity inhibitors may be explained by a tight interaction of the hydrophobic high-affinity cations with several attachment domains at a polyvalent cation binding pocket. Such a type of polyvalent interaction may not allow the replacement of large cations by smaller cations, which may interact with only part of the attachment domains. This hypothesis may also explain why the affinity of the low-affinity cation TMA and of the high-affinity cations MPP and cyanine 863 are not changed by the D475E mutation. These cations may interact with attachment domains of the cation binding pocket that are not affected by the D475E mutation. It is a challenge to determine the amino acid residues that contribute to the cation binding site of rOCT1 and to detect mutations in humans by which the excretion of organic cations is impaired and/or the selectivity of excreted drugs is changed.

## References

- Busch AE, Karch U, Miska D, Gorboulev V, Akhoundova A, Volk C, Arndt P, Ulzheimer JC, Sonders MS, Baumann C, Waldegger S, Lang F and Koepsell H (1998) Human neurons express the polyspecific cation transporter hOCT2, which translocates monoamine neurotransmitters, amantadine, and memantine. *Mol Pharmacol* **54**:342–352.
- Busch AE, Quester S, Ulzheimer JC, Gorboulev V, Akhoundova A, Waldegger S, Lang F and Koepsell H (1996a) Monoamine neurotransmitter transport mediated by the polyspecific cation transporter rOCT1. *FEBS Lett* **395**:153–156.
- Busch AE, Quester S, Ulzheimer JC, Waldegger S, Gorboulev V, Arndt P, Lang F and Koepsell H (1996b) Electrogenic properties and substrate specificity of the polyspecific rat cation transporter rOCT1. *J Biol Chem* **271**:32599–32604.
- Chen B and Przybyla AE (1994) An efficient site-directed mutagenesis method based on PCR. *Biotechniques* **17**:657–659.
- Fykse EM and Fonnum F (1991) Transport of  $\gamma$ -aminobutyrate and L-glutamate into synaptic vesicles. Effect of different inhibitors on the vesicular uptake of neurotransmitters and on the  $Mg^{2+}$ -ATPase. *Biochem J* **276**:363–367.
- Geering K, Theulaz F, Verrey F, Häuptle MT and Rossier BC (1989) A role for the  $\beta$ -subunit in the expression of functional  $Na^+-K^+$ -ATPase in *Xenopus* oocytes. *Am J Physiol* **257**:C851–C858.
- Gründemann D, Gorboulev V, Gambaryan S, Veyhl M and Koepsell H (1994) Drug excretion mediated by a new prototype of polyspecific transporter. *Nature (Lond)* **372**:549–552.
- Ho SN, Hunt HD, Horton RM, Pullen JK and Pease LR (1989) Site-directed mutagenesis by overlap extension using the polymerase chain reaction. *Gene* **77**:51–59.

- Kanai N, Lu R, Satriano JA, Bao Y, Wolkoff AW and Schuster VL (1995) Identification and characterization of a prostaglandin transporter. *Science (Wash DC)* **268**:866–869.
- Kim M-H, Lu M, Lim E-J, Chai Y-G and Hersch LB (1999) Mutational analysis of aspartate residues in the transmembrane regions and cytoplasmic loops of rat vesicular acetylcholine transporter. *J Biol Chem* **274**:673–680.
- Kitayama S, Shimada S, Xu H, Markham L, Donovan DM and Uhl GR (1992) Dopamine transporter site-directed mutations differentially alter substrate transport and cocaine binding. *Proc Natl Acad Sci USA* **89**:7782–7785.
- Koepsell H (1998) Organic cation transporters in intestine, kidney, liver, and brain. *Annu Rev Physiol* **60**:243–266.
- Koepsell H, Gorboulev V and Arndt P (1999) Molecular pharmacology of organic cation transporters in kidney. *J Membr Biol* **167**:103–117.
- Leier I, Jedlitschky G, Buchholz U, Cole SP, Deeley RG and Keppler D (1994) The *MRP* gene encodes an ATP-dependent export pump for leukotriene  $C_4$  and structurally related conjugates. *J Biol Chem* **269**:27807–27810.
- Loo TW and Clarke DM (1999) The transmembrane domains of the human multidrug resistance P-glycoprotein are sufficient to mediate drug binding and trafficking to the cell surface. *J Biol Chem* **274**:24759–24765.
- Meredith D and Boyd CAR (1995) Oligopeptide transport by epithelial cells. *J Membr Biol* **145**:1–12.
- Merickel A, Rosandich P, Peter D and Edwards RH (1995) Identification of residues involved in substrate recognition by a vesicular monoamine transporter. *J Biol Chem* **270**:25798–25804.
- Meyer-Wentrup F, Karbach U, Gorboulev V, Arndt P and Koepsell H (1998) Membrane localization of the electrogenic cation transporter rOCT1 in rat liver. *Biochem Biophys Res Commun* **248**:673–678.
- Müller M and Jansen PLM (1997) Molecular aspects of hepatobiliary transport. *Am J Physiol* **272**:G1285–G1303.
- Nagel G, Volk C, Friedrich T, Ulzheimer JC, Bamberg E and Koepsell H (1997) A reevaluation of substrate specificity of the rat cation transporter rOCT1. *J Biol Chem* **272**:31953–31956.
- Nezu J, Tamai I, Oku A, Ohashi R, Yabuuchi H, Hashimoto N, Nikaido H, Sai Y, Koizumi A, Shoji Y, Takada G, Matsuiishi T, Yoshino M, Kato H, Ohura T, Tsujimoto G, Hayakawa J, Shimane M and Tsuji A (1999) Primary systemic carnitine deficiency is caused by mutations in a gene encoding sodium ion-dependent carnitine transporter. *Nat Genet* **21**:91–94.
- Pourcher T, Zani M-L and Leblanc G (1993) Mutagenesis of acidic residues in putative membrane-spanning segments of the melibiose permease of *Escherichia coli*. I. Effect on  $\text{Na}^+$ -dependent transport and binding properties. *J Biol Chem* **268**:3209–3215.
- Saito H, Masuda S and Inui K-i (1996) Cloning and functional characterization of a novel rat organic anion transporter mediating basolateral uptake of methotrexate in the kidney. *J Biol Chem* **271**:20719–20725.
- Song H, Ming G, Fon E, Bellocchio E, Edwards RH and Poo M (1997) Expression of a putative vesicular acetylcholine transporter facilitates quantal transmitter packaging. *Neuron* **18**:815–826.
- Steiner-Mordoch S, Shirvan A and Schuldiner S (1996) Modification of the pH profile and tetrabenazine sensitivity of rat VMAT1 by replacement of aspartate 404 with glutamate. *J Biol Chem* **271**:13048–13054.
- Tamai I, Ohashi R, Nezu J-i, Yabuuchi H, Oku A, Shimane M, Sai Y and Tsuji A (1998) Molecular and functional identification of sodium ion-dependent, high affinity human carnitine transporter OCTN2. *J Biol Chem* **273**:20378–20382.
- Tamai I, Yabuuchi H, Nezu J-i, Sai Y, Oku A, Shimane M and Tsuji A (1997) Cloning and characterization of a novel human pH-dependent organic cation transporter, OCTN1. *FEBS Lett* **419**:107–111.
- Wilson DM and Wilson TH (1992) Asp-51 and Asp-120 are important for the transport function of the *Escherichia coli* melibiose carrier. *J Bacteriol* **174**:3083–3086.
- Wright SH, Wunz TM and Wunz TP (1995) Structure and interaction of inhibitors with the TEA/ $\text{H}^+$  exchanger of rabbit renal brush border membranes. *Pfluegers Arch* **429**:313–324.
- Wu X, Prasad PD, Leibach FH and Ganapathy V (1998) cDNA sequence, transport function, and genomic organization of human OCTN2, a new member of the organic cation transporter family. *Biochem Biophys Res Commun* **246**:589–595.
- Yamaguchi A, Akasaka T, Ono N, Someya Y, Nakatani M and Sawai T (1992) Metal-tetracycline/ $\text{H}^+$  antiporter of *Escherichia coli* encoded by transposon Tn10. *J Biol Chem* **267**:7490–7498.

---

**Send reprint requests to:** Prof. Dr. Hermann Koepsell, Anatomisches Institut der Universität, Koellikerstrasse 6, D-97070, Würzburg, Germany, E-mail: anat010@mail.uni-wuerzburg.de

---